Iranian Journal of Geophysics, Vol 16 No 4, 2023, Page 85 – 100 (Research Article)
DOI: 10.30499/IJG.2022.343984.1426

Evaluation of GPS RO derived precipitable water vapor against ground-based GPS observations over Iran

Ali Sam Khaniani[1*]

[1] *Assistant Professor, Babol Noshirvani University of Technology, Civil Engineering Department, Mazandaran, Iran*

(Received: 24 May 2022, Accepted: 10 August 2022)

Abstract

For more than two decades, the Global Positioning System (GPS) under a method called GPS meteorology, has been providing valuable products and parameters for meteorologists and climatologists in addition to its main purpose, which is positioning. GPS meteorology can be used in both space-based and ground-based modes. The space-based approach, called GPS Radio Occultation (RO), is used to provide the profiles of refractivity, temperature, pressure, and water vapor pressure in a neutral atmosphere and electron density in the ionosphere. However, ground-based GPS meteorology is utilized to estimate the tropospheric delay of the GPS signals and Precipitable Water Vapor (PWV) value. To date, GPS RO profiles have been used in several researches to study ionosphere and troposphere layers in Iran. However, no studies have yet used these data to estimate and evaluate PWV. In this study, GPS RO profiles were used to calculate and evaluate PWV over the study area. For statistical comparison, ground-based PWV (GB PWV) estimates in 41 stations in the study region have been considered reliable values. After selecting the pair of PWV values obtained from the space-based and ground-based GPS meteorology in the region, statistical parameters were extracted. In general, the results showed that the GPSRO PWV values have 80% correlation with the corresponding values obtained from the ground-based method. The average and RMSE of the GB-GPSRO PWV differences in the region were estimated at 3 mm and 5.2 mm, respectively. Also, the effective parameters on the accuracy of GPSRO PWV values such as seasonal changes, the position of stations, the difference in height of the lowest point of the GPS RO profile from the ground (dh), and the horizontal distance between the profile and the ground station were examined. The correlation of GPSRO PWV and GB PWV for winter, spring, summer, and autumn seasons were estimated at 0.75, 0.72, 0.73, and 0.85, respectively. The reason for the greater correlation between these two methods in the cold seasons of the year can be attributed to the lower variation of PWV values in these seasons. After sensitivity analysis of the factors considered in relation to the quality of GPSRO PWV values, statistical comparison between GB and GPS RO methods was performed using new conditions. The results showed that with dh <500m condition, the MBE and RMSE of GPSRO PWV compare to ground-based method decreased by about 50% and 25%, respectively, and the correlation between these two methods improved by 5%.

Keywords: PWV, GPS RO profiles, ground-based GPS, bias

*Corresponding author: ali.sam@nit.ac.ir

1 Introduction

Water vapor is one of the most important gases in the Earth's atmosphere and has caused more than 65% of the total greenhouse effects. This gas plays an important role in understanding hydrological cycles and climate change. This parameter transfers moisture and latent heat and has a large share in the process of cloud production, precipitation, and flood (Zhai and Eskeridge, 1997; Mazany et al, 2002).

Precipitable Water Vapor (PWV) is one of the most common parameters for expressing water vapor in the atmosphere. If all the available vapor is compressed in a vertical column of the atmosphere, the depth of liquid water in this column is called PWV (Ferrare et al, 2002). Monitoring global PWV changes helps to understand the mechanisms of convective clouds and water vapor transmission (Emardson et al, 1998). This parameter varies greatly at different spatial and temporal scales. Therefore, more accurate PWV measurement is necessary to monitor the spatio-temporal changes of water vapor in order to more accurately predict global climate and weather models (Liang, 2013).

To measure PWV, various methods such as radiosonde, microwave radiometers, ground-based solar photometers, satellite remote sensing observations and GPS meteorology have been used, which have their advantages and disadvantages (Elgered et al, 1997; Neill et al, 2001; Gao et al, 2003; Divakarla et al, 2006; Alexandrov et al, 2009; Whiteman et al, 2012; Sanchez et al, 2013).

Radiosondes are the oldest instrument for measuring atmospheric parameters, which can be used to calculate the PWV values at each station with an accuracy of a few millimeters (Neill et al, 2001). PWV values from radiosondes are considered as a reference for meteorologists. However, the low temporal resolution (twice a day), reduced sensor performance in cold and dry conditions, the high cost, and lack of uniform coverage throughout the land are the limitations of this technique (Pramualsakdikul et al, 2007). Although satellite PWV products have suitable spatial coverage both on land and on water, they have limitations such as low temporal resolution or sensitivity to cloud conditions and the need for calibration.

In 1992, the term "GPS meteorology" was introduced to measure atmospheric water vapor using observations of the ground-based GPS receivers (Bevis et al, 1992) and has quickly gained attention as a powerful tool in the meteorological community. Unique features such as usability in all-weather conditions, long-term stability, continuous observations with a very high temporal resolution, low cost, and high accuracy make this technique another reliable alternative for measuring atmospheric water vapor (Bevis et al, 1994; Pottiaux & Warnant, 2002; Bokoye et al, 2003; Van Baelen et al, 2005; Vey et al, 2010; Vaquero-Martínez et al, 2017).

While observations of ground -based GPS receivers can be used to provide PWV, by solving an inverse problem using observations of GPS receivers mounted on Low Earth Orbit (LEO) satellites, the atmospheric profiles of refractive index, temperature, pressure, and water vapor pressure from the atmosphere can be obtained. The latter method is known as GPS Radio Occultation (GPS RO) (Yuan et al, 1993).

The GPS RO technique can measure the Earth's atmosphere on both water and land (Kursinski et al, 1997) and is more economical than the ground-based GPS meteorology because GPS RO profiles are available for free. On the other hand, the GPS RO technique is not able to provide atmospheric profiles with proper temporal resolution in a fixed location. Also, the lack of retrieval of the atmospheric profiles in the lower layers of the troposphere in severe refraction conditions is another limitation of this method (Fonseca et al, 2018).

Although free GPS RO data complements our information on atmospheric vapor behavior, the accuracy of PWV estimation using GPS RO profiles must be evaluated reliably. On the other hand, ground-based GPS meteorology is one of the most powerful and accurate tools to estimate PWV (Calori et a1, 2016). Therefore, several studies around the world have used ground–based GPS PWV estimates to evaluate the corresponding values obtained from the GPS RO technique.

For example, Teng et al. (2013) compared GPS RO water vapor values derived from the COSMIC satellite observation with the corresponding values of SSM/I and AMSR-E sensors from 2007 to 2011. In their study, the monthly mean values of COSMIC PWV were about 0.98 correlated with the other two sensors, and the RMSE of this statistical comparison was estimated to be about 4 mm. Their results showed that, especially in the tropics, GPS RO water vapor estimates are slightly lower than the corresponding values of SSM/I and AMSR-E sensors. They attributed this to the fact that not all GPS RO profiles reached the ground and have data gaps in the layers near the earth's surface.

Also, Huang et al. (2013) examined the PWV values obtained from the ground-based GPS meteorology technique with GPS RO PWV values from 2007 to 2012 and achieved the correlation coefficient and RMSE of about 0.96 and 3.5 mm, respectively. They also compared monthly mean GPS RO PWV with the corresponding values obtained from NCEP analysis in the northern and southern hemispheres, in areas with few ground stations. They found that the GPS RO in these areas could complement reanalysis models.

In 2018, a study analyzed GPSRO PWV with the help of ground-based GPS PWV in an area surrounded by the ocean. They used 8 years of data from 47 GPS stations to study GPSRO PWV in this region. Comparison of 5000 corresponding data pairs from both methods showed that with a bias of about 1 mm, RMSE about 5 mm, and a correlation of about 0.9, these values are comparable.

So far, several studies have been performed in the Iranian region to evaluate ground-based GPS PWV, applying these values for satellite PWV calibration, assessment of GPS RO profiles, and their use in climate studies (Sharifi et al, 2012 & 2013 & 2016; Khaniani et al, 2020, Khaniani et al, 2021). However, no studies have yet been conducted to estimate GPSRO PWV values in this area. To do this, in this research, PWV values will be calculated using GPS RO profiles in the country and will be evaluated with the help of the corresponding values obtained from ground-based GPS receivers.

The data used and how to calculate PWV values from GPS RO profiles are given in Section 2. In the following, the statistical evaluation process and the method of selecting the corresponding PWV values from both ground-based and space-based methods are described in Section 3. Also, section 4 examines the accuracy of GPSRO PWV compared to ground-based GPS PWV, as well as the factors influencing this statistical evaluation. Finally, the conclusion is presented in Section 5.

2 Data and methodology

The main purpose of this study is to use atmospheric profiles obtained from GPS RO technique to calculate the amount of PWV in the Iranian atmosphere and the next step, the evaluation of these values with the help of ground-based GPS PWV measurements. In the following, the values of PWV resulting from GPS RO profiles and ground- based GPS receivers are called GPSRO PWV and GB PWV, respectively.

2.1 Ground–based GPS PWV

GPS satellite signals pass through the atmosphere before reaching ground-based receivers are bended and delayed. Part of this error is due to the ionosphere layer. Ionosphereic error on the GPS signals can be determined with the help of observations of dual-frequency GPS receivers because the signal delay in this layer depends on the frequency. The rest of the delay is due to the neutral part of the atmosphere, specifically the troposphere, which is not dependent on the signal frequency. Typically, the total tropospheric delay of the GPS signal in the zenith direction (ZTD) along with other unknown coordinate components is estimated during observation processing. This parameter is considered by various meteorological and climatic applications.

ZTD is divided into dry components or Zenith Hydrostatic Delay (ZHD) and Wet Zenith Delay (ZWD). The second part of ZTD depends on atmospheric water vapor (Bevis et al, 1994). Using the pressure values measured at the GPS station, the dry part of the delay can be accurately modeled (Saastamoinen, 1972). ZWD can be obtained by subtracting ZHD from the estimated total delay value (ZTD). Then, using a dimensionless factor that is a function of average atmospheric temperature, the molar mass of dry air and water vapor, and physical constants dependent on atmospheric refraction, ZWD values can be converted to GB PWV using the following equations (Bevis et al, 1994).

$$\mathrm{ZTD} = \mathrm{ZHD} + \mathrm{ZWD} \quad (1)$$

Using the surface pressure measurements P_0 at GPS station, ZHD can be computed accurately through Sasstamoinen model (Davis et al. 1985).

$$\mathrm{ZHD} = \frac{[(0.0022768 \pm 0.0000015)\mathrm{m.hPa^{-1}}]\mathrm{P_0}}{1 - 0.00265\cos(2\varphi) - 0.000285\mathrm{H}} \quad (2)$$

Where φ is the latitude and H is the height from the geoid in kilometers. ZTD is subtracted from ZHD and then ZWD can be achieved easily.

The PWV values are related to the ZWD as follows (Bevis et al. 1994):

$$\mathrm{GB\ PWV} = \frac{10^6}{\rho_w R_v \left[({k_3}/{T_m}) + k_2 + k_1({M_w}/{M_d})\right]} \times \mathrm{ZWD} \quad (3)$$

$M_w(18.0152\ {gr}/{mol})$ and $M_d(28.9644\ {gr}/{mol})$ are the molar mass of water vapor and dry air, respectively. The physical constants $k_1(77.689\ {K}/{hPa})$, $k_2(71.295\ {K}/{hPa})$ and $k_3(375463\ {K^2}/{hPa})$ belong to the formula for atmospheric refractivity (Rüeger, 2002). An empirical relationship was utilized for T_m as a linear function of surface temperature T_0 in Kelvin.

empirical relationship was utilized for T_m as a linear function of surface temperature T_0 in Kelvin.

$$\mathrm{T_m} = 75.39 + 0.7103\ \mathrm{T_0} \quad (4)$$

GB PWV values obtained from the processing of ground-based GPS receiver observations are used as reliable values. In this study, data from 41 permanent GPS stations during 2011, were used to estimate GB PWV values. The details of GPS observation processing and converting ZWD to GB PWV are based on a study by Khaniani et al, (2020). Table 1 lists the geodetic locations of the GPS stations used. Also, the spatial distribution of GPS stations along with the topography of the area is shown in Figure 1.

2.2 GPS RO PWV

GPS and LEO satellites move around the Earth in independent orbits. At certain times, GPS and LEO satellites are on either side of the earth, so that they are not directly in the line of sight, but due to the vertical gradient of the Earth's atmosphere density, the GPS signals are bent and received at receivers onboard the LEO satellite. This event is called GPS Radio Occultation (GPS RO).

Table 1: Geodetic position of permanent GPS stations used in this study.

Station name	Latitude (deg)	Longitude (deg)	Geodetic Height (m)	Geoidal height (m)
abdn	30.37775255	48.21349301	-12.6601	-15.78
abrk	31.12038683	53.22648782	1535.3148	-3.84
absd	35.66112195	52.09116924	1972.6279	1.69
ahar	38.4680734	47.04962779	1360.3417	16.12
ahvz	31.34378063	48.74435648	5.745	-15.17
amnd	38.23110275	46.15520221	1516.7387	17.99
ardh	37.82875217	47.65003405	1774.9576	13.73
baft	29.23909607	56.5800347	2276.1418	-5.35
bebn	30.60556601	50.21695149	302.3242	-13.45
biaj	36.08601935	55.80516683	1091.0112	-9.4
bijd	32.90011422	59.25527201	1475.3756	-12.41
bnab	37.36978084	46.05187676	1302.9064	17.91
bojd	37.48027073	57.2715619	1092.399	-11.91
brmn	37.91895651	47.28837076	1661.3121	15.19
chsm	35.08751651	50.98936447	927.8766	1.42
esfn	37.04945177	57.49456988	1195.126	-12.32
farm	35.69606007	59.8429829	1395.1821	-16.83
ggsh	38.2070034	44.95365208	1314.2339	21.04
gona	34.37300747	58.68353674	1066.8875	-13.98
grgn	36.87568826	54.35325957	4.1848	-8.61
Illm	33.58858181	46.39741896	1327.2232	2.44
kadn	35.59167141	58.8782567	1831.7671	-14.9
klbr	38.88684791	47.17332488	1222.1857	13.67
krad	33.43328533	48.27874015	1158.3291	1.71
lamd	27.3635895	53.20337304	381.1217	-24.52
mavt	37.80091663	55.94384206	442.2135	-14.18
mshn	36.33467048	59.47981627	1087.3832	-16.13
oryh	37.61797382	45.0569518	1356.473	19.94
pold	39.35131236	45.06151352	815.5599	20.26
qqen	33.73988421	59.17603872	1426.7366	-13.22
quch	37.07065024	58.53727065	1323.0495	-14.88
ravr	31.25189103	56.80919583	1179.0583	-8.69
sabz	36.18487699	57.65282767	921.0761	-13.05
safi	36.6980894	57.92127893	1213.267	-13.88
sark	36.5367652	61.14858901	251.5764	-26.75
sfhn	32.51766476	51.70612973	1547.5149	-0.47
shor	35.2771829	51.88422933	946.178	-0.53
shrn	37.43715332	57.82268284	1040.3398	-13.32
tehn	35.69720433	51.33408386	1194.5627	2.68
thed	35.34688662	59.21869476	1460.2244	-15.54
tkbn	36.78585204	50.93004937	-20.6652	1.04

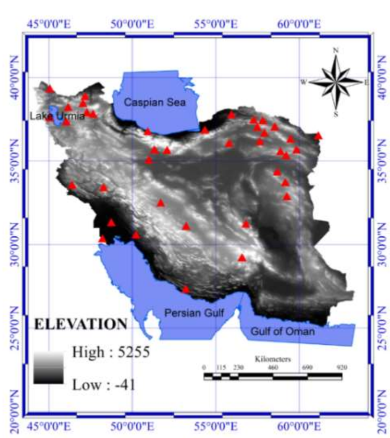

Figure 1. Location of GPS stations (red triangles) used in this study along with topographic changes in the area.

GPS receivers onboard LEO satellites measure the phase and amplitude of signals sent from GPS satellites as a function of time. With accurate information on the position and velocity vectors of both GPS and LEO satellites, it is possible to calculate the excess phase values of the bending signals in the atmosphere, which leads to estimating the bending angle of the GPS signals. (Hajj et al, 2002). After calculating the bending angle profile for both L1 and L2 GPS signals, and using a linear combination of these profiles the ionospheric effect can be removed from the calculated bending angle (Vorob'Ev, 1994). Finally, with the bending angle without the effect of the ionosphere (α (a)), the atmospheric refractive index (n) can be deduced from the following equation (Kursinski et al, 1997).

$$\boldsymbol{n(r) = exp\left[\frac{1}{\pi}\int_x^\infty \frac{\alpha}{\sqrt{a^2 - x^2}} da\right]} \quad (5)$$

In neutral atmosphere, the refractivity (N) is related to geophysical parameters due to the following equation.

$$\mathbf{N = (n-1)\times 10^6 = a_1 \frac{P}{T} + a_2 \frac{\mathit{e}}{T^2}} \quad (6)$$

In equation (6), the coefficients a_1, a_2 are $777.6\ ^{\mathrm{K}}/_{\mathrm{mbar}}$ and $3.73\times 10^5\ ^{\mathrm{K}^2}/_{\mathrm{mbar}}$, respectively. To calculate the values of pressure (P), temperature (T), or water vapor pressure (e) from refractivity, hydrostatic equilibrium and the law of ideal gases are used as additional constraints (Hajj et al, 2002).

$$\mathbf{\frac{dP}{dh} = -g\boldsymbol{\rho}} \quad (7)$$

$$\rho = \rho_\mathrm{d} + \rho_\mathrm{w} = \frac{\mathrm{m_d P}}{\mathrm{TR}} + \frac{(\mathrm{m_w - m_d})e}{\mathrm{TR}} \quad (8)$$

Where g and h are the acceleration of gravity and height and ρ_w, ρ_dd and ρ are the total density, dry air density, and water vapor density, respectively. $\mathrm{m_d}$and $\mathrm{m_w}$ are the average molecular masses of dry air ($28.97\ ^{\mathrm{g}}/_{\mathrm{mole}}$) and water vapor ($18.0\ ^{\mathrm{g}}/_{\mathrm{mole}}$) and R is the universal gas constant. In layers where the water vapor pressure is small, the values of temperature and pressure can be estimated by combining equations (7) and (8) and using equation (6), by solving the system of two unknown equations. However, in the troposphere, where the values of water vapor pressure are important, all three variables of Equation (8) are estimated using variational data assimilation methods (Poli et al, 2002).

Here, The level 2 wetPrf GPS RO profiles provided by the COSMIC Data Analysis and Archive Center (CDAAC) were used which are available in netcdf format at the link https://www.cosmic.ucar.edu/.
Each data file contains the variable pressure, water vapor pressure, temperature and refractivity as a function of altitude above mean sea level. Therefore, by accessing atmospheric profiles, PWV can be calculated using the following equations (Bai, 2005):

$$GPSRO\ PWV = \frac{1}{\rho_w}\int \rho_v\, dh \quad (9)$$

$$GPSRO\ PWV = \frac{1}{\rho_w}\sum(h_{i+1} - h_i)(\rho_v^{i+1} + \rho_v^i)/2 \quad (10)$$

Where $\rho_w = 1025\ ^{\mathrm{kg}}/_{\mathrm{m}^3}$ is the density of liquid water. ρ_v^i is the density of water vapor at the height equal to h_i , which can be calculated based on the equation of state for an ideal gas as follows:

$$\rho_v = \frac{e}{R_v\,.T} \quad (11)$$

Where $\mathrm{R_v} = 461.5\ ^{\mathrm{J}}/_{\mathrm{Kg.\,K}}$ is the constant of gases for water vapor. Water vapor pressure values are present in GPS RO data. In equation (11), T is the absolute temperature in Kelvin. After extracting the required data from each netcdf file, the integral of Equation (9) is solved numerically, and finally, the GPSRO PWV value for each profile is calculated.

In total, 5781 atmospheric profiles obtained from GPS RO measurements of

LEO satellites: COSMIC, GRACE, TerraSAR-X, SACC, and METOP-A during 2011 were used to calculate PWV over Iran. Table 2 shows the number of GPS RO profiles corresponding to each LEO satellite mission.

Table 2. Number of GPS RO profiles used in this study.

GPS RO missions	Number of Profiles
COSMIC	3620
GRACE	240
TerraSAR-X	353
SACC	145
METOP-A	1425
Overall	5781

3 Evaluation Procedure

Initially, GPSRO PWV values were calculated for the entire study period using the equations presented in Section 2. In addition to calculating the GPSRO PWV quantity, location of the profile (geodetic latitude and longitude), time, the height of the lowest point of the GPS RO profile (h_{min}) for all GPS RO profiles were stored in an output file. In later stages, these parameters could be easily used in the statistical comparison of GPSRO PWV concerning the GB PWV values.

After preparing the PWV values obtained from the spaced-based GPS meteorology technique for all GPS RO profiles, it is necessary to select the corresponding values obtained from the processing of ground-based GPS receiver observations (GB PWV). To select suitable GB PWV values for statistical comparison, data with a distance of less than 200 km were used. In other words, if the distance between the ground-based GPS station and the profile location is more than 200 km, the GB PWV values of that station will not be utilized for statistical comparison with GPSRO PWV.

The difference in altitude of the lowest GPS RO data and ground-based GPS station was also considered for statistical comparison. Accordingly, profiles with the lowest data difference in height relative to the ground station height of less than 1 km were selected for statistical comparison. If the h_{min} difference of a profile relative to the height of a GPS station is more than 1000 meters, that profile will be excluded from the statistical comparison. Using the co-location conditions, pairs of GB PWV and GPSRO PWV values were extracted for one year in the Iran region.

To evaluate the accuracy and precision of GPSRO PWV in comparison with one-year GB PWV estimates obtained from 41 ground-based GPS stations, the values of MBE, RMSE, and R were calculated by equations (12) to (14).

$$\mathbf{ME} = \frac{1}{N}\sum_{i=1}^{N}(\mathbf{GB\ PWV_i} - \mathbf{GPSRO\ PWV_i}) \quad (12)$$

$$RMSE = \sqrt{\frac{1}{N}\sum_{i=1}^{N} (\mathrm{GB\ PWV}_i - \mathrm{GPSRO\ PWV}_i)^2} \quad (13)$$

$$R = \frac{\sum_{i=1}^{N} (\mathrm{GB\ PWV}_i - \mathrm{GB\ PWV}_m) \sum_{i=1}^{N} (\mathrm{GPSRO\ PWV}_i - \mathrm{GPSRO\ PWV}_m)}{\sqrt{\sum_{i=1}^{N} (\mathrm{GB\ PWV}_i - \mathrm{GB\ PWV}_m)^2} \sqrt{\sum_{i=1}^{N} (\mathrm{GPSRO\ PWV}_i - \mathrm{GPSRO\ PWV}_m)^2}} \quad (14)$$

N is the total number of pairs of PWV values obtained from GPS RO method and ground-based GPS meteorology. Also, GB PWV_i and GPSRO PWV is the ith values of the PWV time series resulting from the ground-based GPS meteorology and GPS RO technique, respectively. In Equation (10), the subscript m represents the average of the time series of PWV for each station.

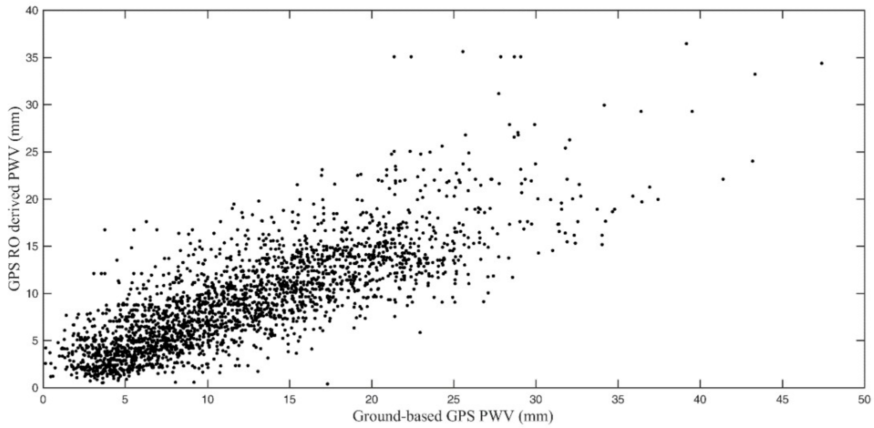

Figure 2. Comparison of GB PWV values with corresponding amounts obtained from GPS RO method in 2011.

4 Results and discussion

4.1 GB PWV and GPS RO PWV comparison

Based on one-year GB PWV values derived from observations of 41 permanent GPS stations and GPSRO PWV obtained from 5781 GPS RO data files, the colocation conditions applied and 2449 pairs of PWV data were prepared. Figure 2 shows the scatter plot of PWV values estimated by GPS RO technique compared to the GB method in Iran.

Based on the results obtained in the study area, the amount of PWV estimated by GPS RO method correlates about 80% with the GB PWV. Also, the mean bias and RMSE of GB-GPSRO PWV differences in the region were estimated at 3 mm and 5.2 mm, respectively. Based on the value of the correlation coefficient, there is a good agreement between the two methods. Given the mean bias value, the GPS RO estimates on average PWV values about 3 mm smaller than those from ground-based GPS meteorology. The reason for this can be attributed to various factors such as the vertical obliquity of GPS RO profiles, lack of GPS RO data in the lowest 1000 meters of the atmosphere, and drastic PWV changes in different places relative to each other. To better understand the reason for the difference between these two methods in estimating PWV, the following factors will be discussed in the statistical comparisons between the ground-based and space-based GPS meteorology.

4.2 Impact of seasonal changes

Since the change of seasons is one of the factors affecting the amount of PWV, in this section, the quality of PWV resulting from the GPS RO technique in terms of statistics such as bias, RMSE, and correlation coefficient in different seasons will be compared and discussed.

In addition to the general comparison made in Figure 2, the GPSRO PWV and GB PWV values in winter (red dots), spring (green dots), summer (blue dots), and autumn (black dots) have been compared separately in Figure 3. According to Figure 3, the correlation of water vapor values obtained from these two methods for winter, spring, summer, and autumn 2011 were estimated 0.75, 0.72, 0.73, and 0.85, respectively. The reason for the greater correlation between these two methods in the cold seasons of the year can be attributed to the lower variation of PWV values in these seasons.

To better understand the relationship between the PWV differences and changing seasons, the seasonal bias and RMSE values of the GB-GPSRO PWV differences for all stations, are drawn in Figures 4 and 5, respectively.

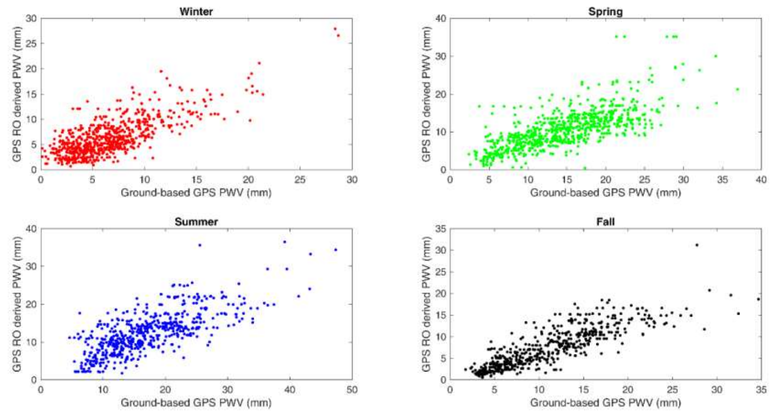

Figure 3. Comparison of estimated PWV values from GPS RO and GB methods in different seasons of 2011.

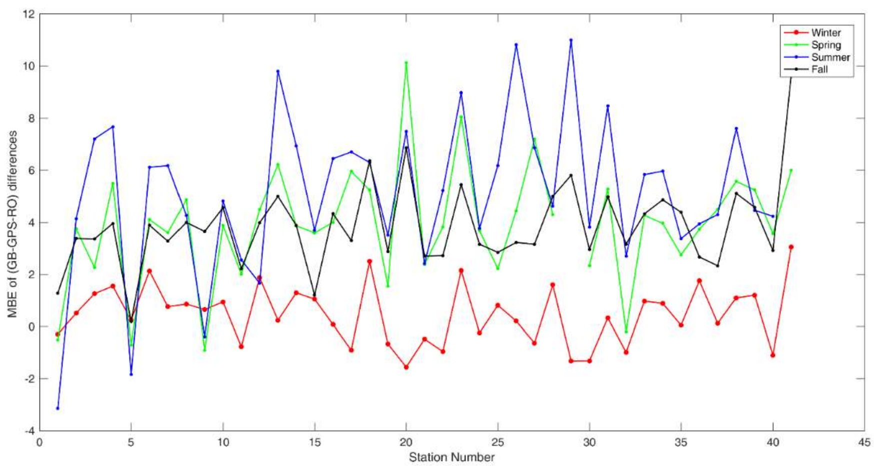

Figure 4. Examining the bias of GB-GPSRO PWV values in different seasons for each GPS station.

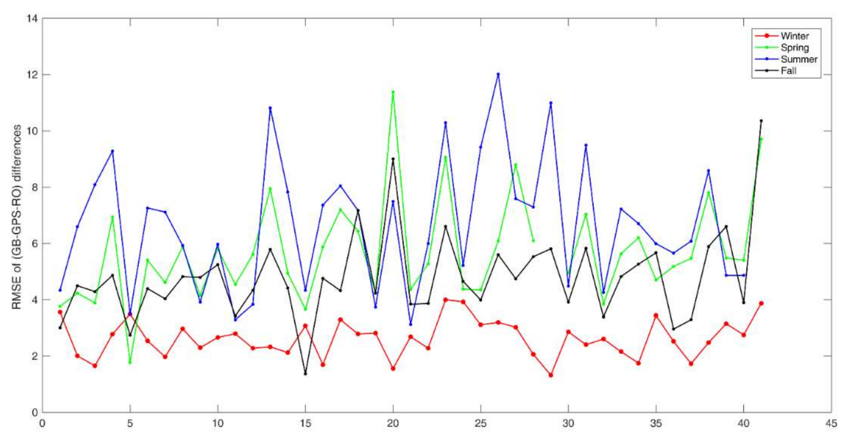

Figure 5. Examining the RMSE of GB-GPSRO PWV values in different seasons for each GPS station.

According to Figure 4, the lowest bias between GPSRO PWV and GB PWV values at all stations can be attributed to winter (red graph), which is estimated about 0.26 mm. Also, the bias between the two methods in autumn and spring is almost the same and the average is about 3 mm. The mean GB-GPSRO PWV bias at all stations was estimated to be around 5 mm for the summer season when water vapor reaches its maximum.

Furthermore, the RMSE of PWV differences between the two methods for winter was lower than other seasons in the study region and was estimated about 2.63 mm. According to Figure 5, the average RMSE values for all stations increase in autumn, spring and summer, subsequently.

Table 3. General comparison of GB PWV and GPSRO PWV obtained from measurements at 41 GPS stations.

Statistic	Mean	Min	Max
MBE	3.3	-0.75	7.34
RMSE	5.3	3.17	9.44
R	0.8	0.63	0.97
N	60	3	126

4.3 Impact of geographical position of station

In this section, we analyze the relationship between the statistical parameters obtained from GPSRO PWV data quality and the geographical location of the stations. The purpose of this study is to understand the association between bias and RMSE of the estimated values with the height, latitude, and longitude of the studied stations. To do this, the average MBE, RMSE, and R statistics of the GPSRO PWV values at each station were calculated. Table 3 provides general statistical results of the accuracy of GPSRO PWV estimates in the region.

Table 4: Correlation between statistical parameters of GB-GPSRO PWV difference values with coordinate components of the studied stations.

Geodetic coordinate / Statistic	Latitude	Longitude	Height
MBE	0.68	-0.01	0.16
RMSE	0.53	0.03	-0.19
R	0.44	-0.30	0.10

According to the results obtained at each station, the GPSRO PWV bias values varied from -0.75 mm to about 7 mm compared to GB PWV in the study area. Also, the range of variation of RMSE values from about 3 mm to 9 mm was obtained. The lowest and highest correlations between GPSRO PWV and GB PWV were estimated to be 0.63 and 0.97, respectively (Table 3).

The correlation between the statistical parameters of the GB-GPSRO PWV difference values with the coordinate components of the GPS stations is given in Table 4. There is a significant positive correlation between the MBE and RMSE values of GPSRO PWV estimates and the latitude of the stations by 0.68 and 0.53, respectively. However, GPSRO PWV statistics had very low correlation with the height and geodetic longitude of the station.

4.4 Impact of minimum height of RO profiles

Besides season and station location, it is important to consider other factors influencing the estimated GPSRO PWV errors. Among these factors can be the horizontal distance between the position of the GPS RO profile and the position of the ground station (**dist**), the height of the lowest data in the profile (**Hmin**), the height difference between the ground station and the lowest point of the GPS RO profile (**dh**) and the time interval between PWV values estimated by the two methods (**dt**). Therefore, the average of the factors mentioned in each station along with the values of MBE, RMSE and correlation coefficient between the selected values of GPSRO PWV and GB PWV are calculated and presented in Table 5. One of the important results in Table 5 is the values of statistics in abdn, ahvz, and bebn stations, which have the lowest bias between GB and GPS RO PWV. The mean bias in these stations is less than 0.75 mm.

The abdn, ahvz, and bebn stations are at low latitudes and, as shown in Table 5, have the lowest bias values for the GB-GPSRO PWV differences. This result is consistent with Table 4 at first glance, because Table 4 already showed a positive correlation of 0.68 between the bias of GPSRO PWV and latitude of the stations. Physically, the RMSE and MBE values were expected to decrease as the latitude of the stations increased, but Table 4 gives the opposite result. Therefore, it is possible that another parameter is effective in increasing the MBE values at high latitude ground stations.

Table 5. Relationship between GB-GPRRO PWV difference values and the average distance between GPS RO profiles and ground station, the time difference between the two methods, the height difference between the ground station and the lowest point of the GPS RO profile, and height of the lowest point of the profile.

Station name	$dist_{mean}$ (Km)	$Hmin_{mean}$ (m)	dh_{mean} (m)	dt_{mean} (min)	MBE (mm)	RMSE (mm)	R	N
abdn	130.68	400.00	396.88	1.25	-0.75	3.70	0.72	70
abrk	139.31	2116.00	583.98	1.34	2.63	4.27	0.75	50
absd	149.17	2264.29	450.25	1.43	3.41	4.75	0.70	28
ahar	139.75	1994.00	724.85	1.20	4.61	6.49	0.86	50
ahvz	135.70	410.42	389.50	1.02	-0.73	3.17	0.82	48
amnd	132.03	2146.81	648.06	1.42	3.67	4.73	0.89	47
ardh	133.75	2266.67	528.57	1.18	3.38	4.78	0.89	99
baft	147.16	2515.84	439.20	3.15	3.43	5.04	0.78	101
bebn	143.99	508.89	300.47	1.33	0.28	3.79	0.81	45
biaj	132.94	1602.06	555.38	1.25	3.59	5.22	0.85	97
bijd	150.23	1791.58	464.19	1.15	1.71	3.68	0.75	95
bnab	113.02	2000.00	715.00	1.28	3.13	4.37	0.85	29
bojd	140.24	1665.69	646.54	1.14	4.93	7.05	0.84	102
brmn	132.97	2237.35	609.02	1.24	3.75	5.04	0.88	83
chsm	99.06	1492.86	588.25	1.50	2.55	3.48	0.91	14
esfn	130.65	1826.32	635.87	1.16	3.89	5.48	0.83	95
farm	138.66	1721.43	523.42	1.16	3.62	6.01	0.72	84
ggsh	140.11	2008.70	715.50	1.26	4.78	5.88	0.88	23
gona	137.79	1530.88	519.61	1.35	1.53	3.74	0.76	68
grgn	163.79	618.18	605.39	1.28	7.34	9.44	0.72	11
illm	125.53	1662.34	575.74	1.26	1.81	3.69	0.78	77
kadn	140.32	2067.46	384.50	1.21	2.73	4.64	0.77	126
klbr	140.04	1832.50	741.54	1.20	6.40	8.18	0.84	40
krad	150.67	1588.57	615.36	1.14	2.71	4.53	0.63	35
lamd	125.39	801.59	507.29	2.79	3.17	6.01	0.81	63
mavt	148.33	787.50	429.60	1.34	3.96	6.76	0.91	48
mshn	154.51	1401.35	608.04	2.96	3.15	5.88	0.69	74
oryh	126.99	2028.57	707.64	1.29	3.48	4.98	0.82	35
pold	110.32	1633.33	838.03	1.33	5.16	7.22	0.97	3
qqen	136.70	1779.59	469.82	1.26	2.00	4.21	0.73	98
quch	133.13	1877.17	625.75	1.03	4.79	6.65	0.84	92
ravr	143.66	1562.22	498.46	1.40	1.17	3.50	0.79	45
sabz	132.28	1586.57	657.46	1.24	3.74	5.22	0.85	67
safi	130.40	1848.19	640.98	1.18	4.06	5.46	0.85	83
sark	126.47	597.14	563.81	2.74	2.21	4.76	0.79	70
sfhn	134.94	2078.38	548.99	1.19	3.01	4.30	0.85	37
shor	150.10	1503.57	581.16	2.25	2.73	4.44	0.86	28
shrn	141.97	1583.56	643.03	1.04	4.69	6.56	0.84	73
tehn	125.23	1740.00	625.52	1.24	3.88	5.01	0.88	25
thed	141.62	1829.79	473.95	1.21	2.25	4.43	0.74	94
tkbn	161.08	583.33	605.04	1.25	7.09	9.00	0.71	12

Table 6. Correlation GB-GPRRO PWV differences and influencing factors in statistical comparison between space-based and ground-based methods of GPS meteorology.

Statistic	$dist_{mean}$	$Hmin_{mean}$	dh_{mean}
MBE	0.20	0.21	0.66
RMSE	0.33	-0.14	0.48
R	-0.58	0.19	0.30

According to Table 5, it can be seen that although the latitude of 3 stations abdn, ahvz and bebn is low, but **dh** is an effective factor in the lower bias of these stations compared to other points. The average values of dh in these points are less than 400 meters. When the value of dh increases in a profile, the lower layers of the atmosphere are not sensed with the GPS RO technique, and the water vapor data of that layers is lost in the PWV calculation. As a result, ground-based GPS meteorology estimate PWV higher than GPSRO at most stations.

To make sure that the reason for the relative increase in MBE values of GPSRO PWV estimates at higher latitudes is not an increase in the latitude component, the correlation between the mean values of **dh** was calculated with the station latitude values. From the results of Table 5, there is a significant correlation between the latitude of the stations and the $\mathbf{dh_{mean}}$ about 0.63. In other words, in stations located at higher latitudes, the mean value of dh was higher than this value in stations located at low latitudes. Therefore, the reason for the higher GPSRO PWV bias in the northern stations of the region was not the increase in the latitude, but the higher average **dh** in the stations.

The correlation coefficient of the error statistics of GPSRO PWV and various factors in all stations is given in Table 6. According to the results, one of the main factors increasing bias in GPSRO PWV estimates compared to GB PWV is the difference between the ground station height and the lowest profile point (**dh**), which has a positive correlation of up to 66% with bias values.

The distance between the GPSRO profile and the GPS station has a weak positive correlation with RMSE and MBE values. Also, the results indicate that increasing horizontal distance reduces the correlation between GPSRO PWV and GB PWV values because the PWV is highly variable in location.

It should be noted that although in some stations, the $\mathbf{dh_{mean}}$ was less than 500 meters, but the height of the lowest profile point in such conditions may have reached 2700 meters. To quantify the effect of **dh** on the evaluation of GPSRO PWV values, among the 2449 GPS RO profiles, those satisfied the **dh <500m** condition were compared with the corresponding ground-based values. As a result, MBE, RMSE, and correlation coefficient between GB PWV and GPSRO PWV were 1.68 mm, 3.95 mm, and 0.85, respectively. Without this condition, the bias between the two methods is about 3 mm and the RMSE is about 5.2 mm and the correlation coefficient is about 80%. Therefore, if the GPS RO profiles up to 500 m above the ground are used to calculate PWV, the average bias and RMSE values can be reduced by about 1.5 mm and 1 mm, respectively. Also, the correlation between GB PWV and GPSRO PWV values is improved by 5%.

By applying the dist <100km condition, the MBE, RMSE, and correlation coefficient of the GPSRO PWV estimates in the region are 3.34 mm, 5.02 mm, and 0.83, respectively. Therefore, as shown in Table 6, reducing the spatial distance did not have much effect on improving the statistics. In addition, the aforementioned statistics for GPSRO PWV by applying the

Hmin <1000m condition are obtained -0.54 mm, 4.44 mm, and 0.82, respectively. Although the reduction of Hmin led to the improvement of bias values, less than the condition dh <500m affects the reduction of RMSE.

Another important point in this study is that the results of this study are based on one-year comparison between GB and GPS RO PWV values. Analyzes long term data at a higher number of ground-based stations to give more general results. However, the values obtained in this study are largely consistent with similar research conducted in other parts of the world.

It should be noted that GPS RO profiles are skewed in height. To clarify this, Figure 6 represents the three-dimensional position of data points in an arbitrary GPS RO profile. As shown in Figure 6, the geodetic latitude of the profile points starts about 40.7° at the lowest point and reaches about 39.9° at an altitude of 40 km. Also, the values of the geodetic longitude of the lowest point and the highest point of the profile are 57.76° and 57.65°, respectively. Therefore, the top and bottom of the profile belong to a horizontal range of about 100 km. On the other hand, in the ground-based method GPS meteorology, the amount of PWV is estimated in the column of air above a GPS station, which geometrically shows the difference between the two methods. Therefore, part of the discrepancy in PWV values from the two methods is due to differences in the geometry of these techniques and should not be considered a mere error due to the GPS RO technique.

5 Conclusion

Water vapor is one of the most important parameters in the study of climate change. There are several methods to estimate this parameter. GPS meteorology technique is one of these methods. This technique is used in both space-based and ground-based modes in meteorology and climatology. In the space-based mode called the GPS RO method, meteorological profiles, including pressure, water vapor pressure, temperature, and refractive index are provided to researchers. In this study, based on one-year of PWV values estimated in 41 permanent ground-based GPS stations in Iran, an attempt was made to evaluate the PWV values obtained from GPS RO profiles. The following is a summary of the most important results obtained from this research.

- Given the distance of less than 200 km between the profile and the ground station, as well as the use of profiles whose lowest point was less than 1 km from the GPS station, the pair of GB PWV and GPSRO PWV values were chosen. According to the results, GPSRO PWV was up to 80% correlated with the ground-based GB PWV. According to the mean bias value, the GPS RO technique estimates PWV values on average about 3 mm lower than the ground-based method. Also, the average RMSE of GB-GPSRO PWV differences in the region was estimated at 5.2 mm.
- Seasonal comparison between GPSRO PWV and GB PWV in 2011 showed that the correlation of water vapor values obtained from these two methods in the study region for winter, spring, summer, and autumn seasons are 0.75, 0.72, 0.73, and 0.85, respectively. The greater correlation between these two methods in the cold seasons of the year can be attributed to the lower PWV value in these seasons. In addition, the RMSE of PWV differences between the two methods for winter was lower than in other seasons and was estimated about 2.63 mm.

In addition, the relationship between GPSRO PWV statistics and various factors including the mean spatial distance between the GPS RO profile and the ground station, the difference between the ground station height and the lowest profile point, and the height of the lowest profile point were investigated. The results showed that one of the main factors increasing RMSE and bias in GPSRO PWV estimates compared to GB PWV is the difference in ground station height and the lowest profile point (**dh**), which has a positive correlation of up to 66% with bias values. Also, as the distance between the ground station and the GPS RO profile increases, the correlation decreases between the GPSRO PWV and GB PWV values.

- After sensitivity analysis of the abovementioned factors in relation to the quality of GPSRO PWV values, statistical comparison between the two methods was performed using new filters in selecting the pair of corresponding PWV values. By applying dh <500m in the selection of GPS RO profiles, MBE, RMSE, and correlation coefficient between GB PWV and GPSRO PWV were obtained 1.68 mm, 3.95 mm, and 0.85, respectively. Considering the condition: dist <100Km, the values of MBE, RMSE, and correlation between the two methods were obtained 3.34 mm, 5.02 mm, and 0.83, respectively. Finally, by applying the Hmin <1000m condition, the values of MBE, RMSE, and the correlation between GB PWV and GPSRO PWV were -0.54 mm, 4.44 mm, and 0.82, respectively. Therefore, it can be recommended that to use GPSRO PWV values in related studies, it is better to use profiles that have a gap of less than 500 meters to the surface.

References

Alexandrov, M. D., Schmid, B., Turner, D. D., Cairns, B., Oinas, V., Lacis, A. A., Gutman, S. I., Westwater, E. R., Smirnov, A., Eilers, J., 2009, Columnar water vapor retrievals from multifilter rotating shadowband radiometer data. J. Geophys. Res. Atmos. 114.

Bai, Z., 2005, Near-real-time GPS sensing of atmospheric water vapor.PhD thesis, Queensland University of Technology

Bevis, M., Businger, S., Herring, T. A., Rocken, C., Anthes, R. A., Ware, R. H., 1992, GPS meteorology - Remote sensing of atmospheric water vapor using the Global Positioning System. J. 97, 15787-15801.

Bevis, M., Businger, S., Chiswell, S., Herring, T. A., Anthes, R. A., Rocken, C., Ware, R. H., 1994, GPS Meteorology: Mapping Zenith Wet Delays onto Precipitable Water. J. Appl. Meteorol. 33, 379-386.

Bokoye, A. I., 2003, Multisensor analysis of integrated atmspheric water vapor over Canada and Alaska. J. Geophys. Res. 108.

Calori, A., Santos, J., Blanco, M., Pessano, H., Llamedo, P., Alexander, P. and de la Torre, A., 2016, “Ground-based GNSS network and integrated water vapor mapping during the development of severe storms at the Cuyo region (Argentina)”, Atmos. Res., 176, 267-275.

Divakarla, M. G., Barnet, C. D., Goldberg, M. D., McMillin, L. M., Maddy, E., Wolf, W., Zhou, L., Liu, X., 2006, Validation of atmospheric infrared sounder temperature and water vapor retrievals with matched radiosonde measurements and forecasts. J Geophys Res 111, D09S15. doi:10.1029/2005JD006116

Davis, J. L., Herring, T. A., Shapiro, I. I., Rogers, A. E. E., Elgered, G., 1985, Geodesy by radio interferometry: Effects of atmospheric modeling errors on estimates of baseline length. Radio Sci Vol. 20, Issue 6, pages 1593–1607

Elgered, G., Johansson, J. M., Rönnäng, B. O., Davis, J. L., 1997, Measuring regional atmospheric water vapor using the Swedish permanent GPS network. Geophys. Res. Lett. 24, 2663-2666.

Emardson, T. R., Elgered, G. and Johansson, J. M., 1998, Three months of continuous monitoring of atmospheric water vapor with a network of Global Positioning System receivers, J. Geophys. Res., 103, 1807–1820.

Ferrare, R., Brasseur, L., Clayton, M., Turner, D., Remer, L., Gao, B. C., 2002, Evaluation of terra aerosol and water vapor measurements using ARM SGP data. 11th Conf. Atmos. Radiat. 130–133.

Fonseca, Y. B., Alexander, P., de la Torre, A., Hierro, R., LLamedo, P. and Calori, A., 2018, Comparison between GNSS ground-based and GPS radio occultation precipitable water observations over ocean-dominated regions. Atmospheric Research, 209, 115-122.

Gao, B. C., Yang, P., Guo, G., Park, S. K., Wiscombe, W. J., Chen, B., 2003, Measurements of water vapor and high clouds over the Tibetan Plateau with the Terra MODIS instrument. IEEE Trans. Geosci. Remote Sens. 41, 895-900.

Hajj, G. A., Kursinski, E., Romans, L., Bertiger, W., Leroy, S. J. J. o. A. and Physics, S.-T., 2002, 'A technical description of atmospheric sounding by GPS occultation', 64(4), 451-469.

Huang, C. Y., Teng, W. H., Ho, S. P. and Kuo, Y. H., 2013, Global variation of COSMIC precipitable water over land: Comparisons with ground-based GPS measurements and NCEP reanalyses. Geophysical Research Letters, 40(19), 5327-5331.

Khaniani, A. S., Nikraftar, Z. and Zakeri, S., 2020, Evaluation of MODIS Near-IR water vapor product over Iran using ground-based GPS measurements. Atmospheric Research, 231, 104657.

Khaniani, A. S., Motieyan, H. and Mohammadi, A., 2021, Rainfall forecast based on GPS PWV together with meteorological parameters using neural network models. Journal of Atmospheric and Solar-Terrestrial Physics, 214, 105533.

Kursinski, E., Hajj, G., Schofield, J., Linfield, R. and Hardy, K. R. J. J. o. G. R. A., 1997, 'Observing Earth's atmosphere with radio occultation measurements using the Global Positioning System', 102(D19), 23429-23465.

Liang, J., 2013, Chemical Modeling for Air Resources Fundamentals, Applications, and Corroborative Analysis. Academic Press, Boston, pp. 143-161.

Mazany, R. A., Businger, S., Gutman, S. I., Roeder, W., 2002, A Lightning Prediction Index that Utilizes GPS Integrated Precipitable Water Vapor*. Weather Forecast. 17, 1034-1047.

Niell, A. E., Coster, A. J., Solheim, F. S., Mendes, V. B., Toor, P. C., Langley, R. B., Upham, C. A., 2001, Comparison of measurements of atmospheric wet delay by radiosonde, water vapor radiometer, GPS, and VLBI. J. Atmos. Ocean. Technol. 18, 830-850.

Poli, P., Joiner, J. and Kursinski, E. R., 2002, 1DVAR analysis of temperature and humidity using GPS radio occultation refractivity data. Journal of Geophysical Research: Atmospheres, 107(D20), ACL-14.

Pottiaux, E., Warnant, R., 2002, First comparisons of precipitable water vapor estimation using GPS and water vapor radiometers at the Royal Observatory of Belgium. GPS Solut. 6(1-2), 11-17.

Pramualsakdikul, S., Haas, R., Elgered, G., Scherneck, H. G., 2007, Sensing of diurnal and semi-diurnal variability in the water vapour content in the tropics using GPS measurements. Meteorol. Appl. 14, 403-412.

Rüeger, J. M., 2002, Refractive index formula for radio waves. Integration of techniques and corrections to achieve accurate engineering. Proceedings of the XXII FIG Intional Congress ACSM/SPRS Annual Conference, Washington, DC, USA, 19–26

Sánchez, J. L., Posada, R., García-Ortega, E., López, L., Marcos, J. L., 2013, A method to improve the accuracy of continuous measuring of vertical profiles of temperature and water vapor density by means of a ground-based microwave radiometer. Atmos. Res. 122, 43-

54.

Saastamoinen, J., 1972, Atmospheric Correction for the Troposphere and Stratosphere in Radio Ranging Satellites. In Geophysical Monograph Series; American Geophysical Union: Washington, DC, USA; Volume 15, pp. 247–251.

Sharifi, M. A., Safari, A., Masoumi, S. and Khaniani, A. S., 2012, Harmonic analysis of the ionospheric electron densities retrieved from FORMOSAT-3/COSMIC radio occultation measurements. Advances in space research, 49(10), 1520-1528.

Sharifi, M. A., Sam Khaniani, A., Masoumi, S., Schmidt, T. and Wickert, J., 2013, Least-squares harmonic estimation of the tropopause parameters using GPS radio occultation measurements. Meteorology and Atmospheric Physics, 120(1), 73-82.

Sharifi, M. A., Azadi, M. and Khaniani, A. S., 2016, Numerical simulation of rainfall with assimilation of conventional and GPS observations over north of Iran. Annals of Geophysics, 59(3), P0322-P0322.

Teng, W. H., Huang, C. Y., Ho, S. P., Kuo, Y. H. and Zhou, X. J., 2013, Characteristics of global precipitable water in ENSO events revealed by COSMIC measurements. Journal of Geophysical Research: Atmospheres, 118(15), 8411-8425.

Van Baelen, J., Aubagnac, J. P., Dabas, A., 2005, Comparison of near-real time estimates of integrated water vapor derived with GPS, radiosondes, and microwave radiometer. J. Atmos. Ocean. Technol. 22, 201-210.

Vaquero-Martínez, J., Antón, M., de Galisteo, J. P. O., Cachorro, V. E., Costa, M. J., Román, R., Bennouna, Y. S. 2017, Validation of MODIS integrated water vapor product against reference GPS data at the Iberian Peninsula. International journal of applied earth observation and geoinformation, 63, 214-221

Vey, S., Dietrich, R., Rülke, A., Fritsche, M., Steigenberger, P. and Rothacher, M., 2010, Validation of precipitable water vapor within the NCEP/DOE reanalysis using global GPS observations from one decade. Journal of Climate, 23(7), 1675-1695.

Vorob'Ev, V. V., 1994, Estimation of the accuracy of the atmospheric refractive index recovery from Doppler shift measurements at frequencies used in the NAVSTAR system. Atmos. Ocean. Phys., 29, 602-609.

Whiteman, D. N., Cadirola, M., Venable, D., Calhoun, M., Miloshevich, L., Vermeesch, K., Twigg, L., Dirisu, A., Hurst, D., Hall, E., Jordan, A., Vömel, H., 2012, Correction technique for Raman water vapor lidar signal-dependent bias and suitability for water vapor trend monitoring in the upper troposphere. Atmos. Meas. Tech. 5, 2893-2916.

Yuan, L., Anthes, R. A., Ware, R. H., Rocken, C., Bonner, W. D., 1993, M. G. Bevis and S. Businger, Sensing Climate Change Using the Global Positioning System, Journal of Geophys. Res., Vol. 98, No. D8, pp 14,925-14,937.

Zhai, P., Eskridge, R. E., 1997, Atmospheric water vapor over China. J. Clim. 10, 2643-2652.